

Two-Proton Correlations near Midrapidity in $p + Pb$ and $S + Pb$ Collisions at the CERN SPS

H. Bøggild¹, J. Boissevain², L. Conin³, J. Dodd⁴, B. Erasmus³, S. Esumi^{5,a}, C.W. Fabjan⁶, D.E. Fields^{2,b}, A. Franz^{6,c}, K.H. Hansen^{1,†}, E.B. Holzer⁶, T.J. Humanic⁷, B.V. Jacak⁸, R. Jayanti^{7,9}, H. Kalechofsky^{7,9}, Y.Y. Lee^{7,9}, M. Leltchouk⁴, B. Lörstad¹⁰, N. Maeda^{5,d}, L. Martin³, A. Medvedev⁴, A. Miyabayashi¹⁰, M. Murray¹¹, S. Nishimura^{5,e}, G. Paic^{3,f}, S.U. Pandey^{7,9,g}, F. Piuz⁶, J. Pluta^{3,h}, V. Polychronakos¹², M. Potekhin⁴, G. Poulard⁶, A. Sakaguchi^{5,i}, M. Sarabura², J. Schmidt-Sørensen¹⁰, M. Spegel⁶, J. Simon-Gillo², W. Sondheim², T. Sugitate⁵, J.P. Sullivan², Y. Sumi⁵, H. van Hecke², W.J. Willis⁴, K. Wolf^{11,†} and N. Xu^{2,j}

(The NA44 Collaboration)

¹ Niels Bohr Institute, DK-2100 Copenhagen, Denmark.

² Los Alamos National Laboratory, Los Alamos, NM 87545, USA.

³ SUBATECH, Nantes 44070, France.

⁴ Columbia University, New York, NY 10027, USA.

⁵ Hiroshima University, Higashi-Hiroshima 724, Japan.

⁶ CERN, CH-1211 Geneva 23, Switzerland.

⁷ Ohio State University, Columbus, OH 43210, USA.

⁸ SUNY Stony Brook, Stony Brook, NY 11794, USA.

⁹ University of Pittsburgh, Pittsburgh, PA 15260, USA.

¹⁰ University of Lund, S-22362 Lund, Sweden.

¹¹ Texas A&M University, College Station, TX 77843, USA.

¹² Brookhaven National Laboratory, Upton, NY 11973, USA.

^a Now at Heidelberg University, Heidelberg, D-69120, Germany.

^b Now at University of New Mexico, Albuquerque, NM 87185, USA.

^c Now at Brookhaven National Laboratory, Upton, NY 11973, USA.

^d Now at Florida State University, Tallahassee, FL 32306, USA.

^e Now at University of Tsukuba, Ibaraki 305, Japan.

^f Now at Ohio State University, Columbus, OH 43210, USA.

^g Now at Wayne State University, Detroit, MI 48201, USA.

^h Permanent address: Warsaw University of Technology, Koszykowa 75, 00-662 Warsaw, Poland.

ⁱ Now at Osaka University, Osaka 560, Japan.

^j Now at Lawrence Berkeley National Laboratory, Berkeley, CA 94720, USA.

[†] Deceased.

Abstract

Correlations of two protons emitted near midrapidity in $p + Pb$ collisions at 450 GeV/ c and $S + Pb$ collisions at 200A GeV/ c are presented, as measured by the NA44 Experiment. The correlation effect, which arises as a result of final state interactions and Fermi-Dirac statistics, is related to the space-time characteristics of proton emission. The measured source sizes are smaller than the size of the target lead nucleus but larger than the sizes of the projectiles. A dependence on the collision centrality is observed; the source size increases with decreasing impact parameter. Proton source sizes near midrapidity appear to be smaller than those of pions in the same interactions. Quantitative agreement with the results of RQMD (v1.08) simulations is found for $p + Pb$ collisions. For $S + Pb$ collisions the measured correlation effect is somewhat weaker than that predicted by the model simulations, implying either a larger source size or larger contribution of protons from long-lived particle decays.

PACS codes: 13.60.Rj; 13.85.-t; 25.75.-q; 25.75.Gz

Keywords: two-proton correlations; proton-nucleus, nucleus-nucleus; heavy-ion collisions; proton source size; CERN SPS

1 Introduction

Correlations of identical particles emitted with similar velocities are commonly used as a tool to measure the space-time development of the emission process in particle and heavy-ion collisions. The technique is most often used for bosons, for which the effect of quantum (Bose-Einstein) statistics is the only source of correlations (photons), or plays a dominant role (pions and kaons). Other effects, in particular those due to the Coulomb interaction for pairs of charged particles, are usually treated as a correction. In the case of protons, final state interactions, due to strong and Coulomb forces, typically dominate the effect of quantum statistics and determine the form of the correlation function. A negative correlation effect, due to Fermi-Dirac statistics and Coulomb repulsion, competes with the positive (attractive) correlation due to the strong interaction, giving rise to a characteristic “dip-peak” structure (minimum at zero, maximum at ≈ 20 MeV/ c proton momentum in the pair rest frame) in the two-proton correlation function. The height of the correlation peak decreases as the proton source size increases. All effects are strongly sensitive to the space-time parameters of the emission process [1, 2, 3, 4].

Correlations of protons emitted with small relative momenta were observed for the first time in $\pi^- + Xe$ interactions at 9 GeV/ c [5]. Currently, two-proton correlations are used extensively in low energy (of order 10-1000 MeV/ c) heavy-ion physics [6, 7, 8, 9] where the sizes measured for small proton momenta are comparable to or exceed the size of the larger (usually target) nucleus. A similar result was obtained at much higher CERN SPS energies in the target fragmentation region, where a two-proton correlation analysis yielded source sizes compatible with the sizes of the target nuclei [10]. A decrease of the measured size with increasing proton momenta is reported in many papers however, and for very different projectile energies [6, 7, 9, 11, 12]. Several authors have also reported a dependence on collision impact parameter in low energy heavy-ion interactions [8, 13]. The observed trends in the measured sizes may be related to differences in the proton emission time [7, 9], and may also reflect the reaction dynamics, which can produce correlations between the momentum and position of the emitted particles [14].

In spite of extensive analysis of pion and kaon correlations in relativistic heavy-ion collisions, data for two-proton correlations are scarce. This paper reports the first measurement of proton-proton correlations at midrapidity at CERN SPS energies. The origin of protons emitted in relativistic heavy-ion collisions differs from that of lighter particles. Protons are constituent parts of the projectile and target nuclei, unlike pions and kaons which are produced in the collision. The different dynamics of proton emission may therefore be reflected in different source sizes. At the SPS, the expected net baryon-free region at midrapidity for the highest collision energies is not yet achieved. There is still significant stopping, with the associated rapidity shifts of projectile and target nucleons leading to an increase in the proton density at midrapidity [15, 16]. Consequently, the ratio of antiprotons to protons at midrapidity is approximately 0.1 [15]. The relatively high degree of stopping implies that secondary interactions of pions, kaons and other produced particles with nucleons are important, and may influence the size of the proton emission region. The relation between the proton source

size, the dimensions of the colliding nuclei, and the corresponding source sizes for pions and kaons at midrapidity for CERN SPS energies is still an open question. In this context, the results of the two-proton correlation analysis described here provide complementary information to existing data from two-boson correlations which can be useful in understanding the underlying dynamics of the collisions [17, 18, 19, 20, 21, 22].

The paper presents the results of a proton-proton correlation analysis for collisions of two different projectiles, protons and sulphur nuclei, with a lead target. In the first case, the projectile consists of a single proton, and the measured pairs contain mainly protons from the target or protons produced in the interaction. In the second case, the correlated pairs contain both projectile and target participants as well as produced protons. The relative role of these different sources will depend on the impact parameter of the collisions, i.e. the centrality selection. This dependence is examined by an analysis of the correlation effects as a function of charged particle multiplicity in the collision. Finally, the experimental correlation functions are compared to predictions obtained from both a Gaussian source model and from the RQMD event generator, version 1.08 [23].

2 Experiment

The NA44 detector is described in [17]. The spectrometer is optimized to measure single- and two-particle distributions of charged hadrons produced near midrapidity in pA and AA collisions. The momentum acceptance is $\pm 20\%$ of the nominal momentum setting, and only particles of a fixed charge sign are detected for a given spectrometer setting.

The data used for this analysis were taken at the 6 GeV/ c setting with the spectrometer axis at 44 mrad with respect to the incident beam. The corresponding acceptance for protons is $2.35 < y < 2.70$ and $0.0 < p_T < 0.66$ GeV/ c ($\langle p_T \rangle \approx 230$ MeV/ c). Scintillator hodoscopes are used for tracking, and also provide time-of-flight information with $\sigma_{\text{TOF}} < 100$ ps. The momentum resolution $\delta p/p$ is approximately 0.2%. Two threshold Cerenkov detectors in conjunction with the time-of-flight (mass-squared) information provide particle identification. Particle contamination is less than 1% for the data shown here. An interaction trigger is provided by two rectangular scintillator paddles sitting downstream of the target and covering approximately $1.3 < \eta < 3.5$. Offline, a silicon pad multiplicity detector with 2π azimuthal coverage over the range $1.5 < \eta < 3.3$ is used for event characterization.

Target thicknesses of 10mm and 5mm were used for the $p+Pb$ and $S+Pb$ data, corresponding to approximately 5.9% and 5.0% interaction lengths respectively. Multiple scattering in the targets, combined with the spectrometer momentum resolution, lead to a resolution in k^* , the particle momentum in the rest frame of the pair, of $\sigma(\delta k^*) \approx 9$ MeV/ c . The experimental trigger required an interaction in the target, at least two tracks in the spectrometer, and a veto on pions (and lighter particles) in the spectrometer acceptance. No centrality selection was made in the trigger, however the two-track requirement itself biases the data towards high-multiplicity events. Offline track reconstruction was followed by track quality cuts, including rejection of close-by tracks, and particle identification cuts to select proton pairs. Additional

cuts to reject multiple interactions in the target (pileup) and require clean events were made. The final event samples are approximately 8k pairs for the $p + Pb$ data and 15k pairs for the $S + Pb$ interactions.

3 Correlation Analysis

The experimental correlation function is constructed from identified two-proton events. Due to limited statistics, only a one-dimensional analysis has been performed. The correlation function is calculated as:

$$C(k^*) = \frac{N_{corr}(k^*)}{N_{uncorr}(k^*)} \quad (1)$$

where k^* is the particle momentum in the rest frame of the pair: $k^* = \frac{\sqrt{-Q^2}}{2}$, $Q \equiv \{q_0, \vec{q}\} = p_1 - p_2$ and p_1, p_2 are the particle 4-momenta. The correlated, N_{corr} , and uncorrelated, N_{uncorr} , proton pairs are taken from the same and different events respectively. The stability of the resulting correlation function under the applied cuts is studied by varying each cut (such as the mass-squared selection, and the hodoscope multiplicity) individually. In all cases, the correlation function data points are within one standard deviation of their nominal values. The stability with respect to different sampling procedures for producing the mixed-event distribution is also tested, and introduces no systematic deviations.

The experimental correlation functions presented here do not contain any correction factors. Such corrections are often made in boson correlation measurements to take account of the effects of finite detector acceptance and momentum resolution, residual correlations in the background distribution [24], and the Coulomb interaction, thereby recovering the “ideal” correlation function in which correlations are due purely to quantum statistics. Rather than correct the experimental distributions, theoretical correlation functions based on model predictions have been generated, and modified to include each of these effects. The results of these simulations are then compared directly to the measured correlation functions.

The theoretical correlation function is generated by selecting proton pairs from a given source model, calculating the associated weight due to quantum statistics and final state interactions (strong and Coulomb) [2, 3], and propagating the particles through a realistic simulation of the experimental detector, including all instrumental and acceptance effects. A full calculation of Coulomb effects is used rather than the Gamow factor approximation. Data cuts are then made in exactly the same way as for the experimental data. For this analysis, two models have been used as inputs for the simulation: a Gaussian source model and the RQMD event generator.

In the case of the Gaussian model, a Gaussian density distribution $\rho(\vec{r}, t) = \frac{1}{(2\pi)^2 r_0^3 \tau} e^{-\frac{\vec{r}^2}{2r_0^2} - \frac{t^2}{2\tau^2}}$ is assumed for both the spatial and temporal extent of the source [2]. It is assumed that protons are emitted by sources moving in the longitudinal direction with the velocities of the proton pairs (the Longitudinally Co-moving Source, LCMS). In this way the fast longitudinal

motion of proton sources at mid-rapidity is taken into account. Because the rapidity acceptance in this measurement is narrow ($2.35 < y < 2.70$), the results assuming the LCMS should not differ significantly from the results assuming a fixed frame of reference centered at about $y = 2.5$. Since a one-dimensional analysis is performed here, a spherically-symmetric source parametrized by equal r_o radius and τ time parameters is assumed. The RMS radius in this parametrization is given by $\sqrt{3}r_o$.

In order to compare with RQMD predictions, the theoretical correlation function for pairs of protons from generated events is calculated [3], and the appropriate weighting for different impact parameter collisions is taken into account by matching the multiplicity distributions of the data and model. This matching shows that, in contrast to the $p + Pb$ data where only the highest multiplicity events are selected by the trigger, the $S + Pb$ data are only weakly biased toward central collisions.

In calculating correlation functions for comparison to data, three factors are particularly important: the admixture of indirect protons coming from hyperon (mainly $\Lambda \rightarrow \pi^- p$) decays, the acceptance and resolution of the experiment, and the residual correlations arising in the single particle background distributions.

Weak decays of strange baryons are a significant source of protons and contribute to the yields measured in the NA44 spectrometer. The influence of the admixture of indirect protons on the shape of correlation function has been studied using data from the RQMD and Venus (v5.21) [25] event generators, combined with a detailed simulation (GEANT) of the detector. The two models give similar results: about 22% of protons measured in the spectrometer come from the decay of Λ 's in both $p + Pb$ and $S + Pb$ collisions, and cannot be distinguished from direct protons. This contribution has only a weak p_T dependence, and is greater at low p_T . In order to take into account this non-correlated contribution to coincident pairs, a fraction of 22% of “decay” protons is included when calculating the correlation function, giving about 39% of uncorrelated pairs in the two-particle sample. These pairs are assigned a weight of unity in the correlation function calculation. This contribution significantly reduces the magnitude of the observed correlation effect, but does not change the general shape of the correlation function.

The acceptance and resolution of the NA44 spectrometer for protons is estimated using a detailed simulation of the detector, including systematic effects introduced by the track reconstruction procedure for close-by pairs of particles. The k^* acceptance for proton pairs is convoluted with the detector resolution and the rather complicated shape of the two-proton correlation function, and gives rise to an asymmetric distortion of the correlation peak. This “smearing” is particularly important for small k^* , where the expected depletion due to Coulomb and statistical effects is masked by the experimental resolution.

Residual correlations arise in the mixing procedure because the single particle distributions forming the reference (background) sample are in fact projections of the measured two-particle distribution, which includes the correlations. This effect is taken into account by calculating and applying weights which correspond to the mean value of the correlation function for all combinations of a given particle with all others [24]. This residual correlation modifies slightly the height of the correlation peak, and induces a slope for large values of k^* .

All three effects are included in the simulation procedure. In Fig. 1 they are demonstrated separately in order to illustrate their particular features and the relative significance of each of them.

4 Results

The experimental proton-proton correlation functions for $p + Pb$ and $S + Pb$ collisions are presented in Fig. 2. The correlation functions have been normalized such that $C(k^*) = 1$ for $80 < k^* < 160$ MeV/ c . The peak observed in the region of small k^* values (≈ 20 MeV/ c) can be attributed to the combined effect of the final state interaction and Fermi-Dirac statistics. It reflects the space-time properties of the proton emission process. The two correlation functions have qualitatively the same shape, but the peak is much more pronounced for the $p + Pb$ data than for the $S + Pb$, indicating that protons are emitted from a smaller source in the case of $p + Pb$ collisions. Also shown are the correlation functions and associated source sizes from the Gaussian model obtained with a minimum- χ^2 fit over the range $0 < k^* < 160$ MeV/ c . The fits yield $r_o = \tau = 1.42_{-0.05}^{+0.04}$ fm ($\chi^2/N_{DF} = 10.3/10$) for $p + Pb$ and $r_o = \tau = 2.65_{-0.09}^{+0.09}$ fm ($\chi^2/N_{DF} = 9.6/10$) for the $S + Pb$ data. (Note that the r_o values have to be multiplied by $\sqrt{3}$ to obtain the corresponding RMS radii.) Fits assuming $\tau = 0$ give r_o parameters which are equal within errors to those obtained with $\tau = r_o$. This is a consequence of the weak time dependence of the final state interaction effects for small particle velocities [2]; for these data the mean velocity of the proton pairs in the LCMS frame is $\approx 0.24c$.

These results have been obtained assuming that the fraction of measured protons from Λ decay is that given by the simulations described above (22%). While the RQMD and Venus models give consistent results for the fraction of protons from hyperon decays in the NA44 acceptance, there is a factor of order two discrepancy between the available experimental data on Λ production yields in $S + A$ collisions at CERN SPS energies [26, 27]. The RQMD prediction is roughly midway between the two measurements. Using the experimental data as an estimate of the uncertainty on the Λ yield (approx. $\pm 40\%$), and hence on the fraction of protons from Λ decays, gives $r_o = \tau = 1.42_{-0.17}^{+0.16}$ fm for $p + Pb$ and $r_o = \tau = 2.65_{-0.17}^{+0.19}$ fm for $S + Pb$. The RMS radii of the proton and the sulphur and lead nuclei are 0.88 fm, 3.26 fm and 5.50 fm respectively [28]. In the frame of this geometrical interpretation, the measured source sizes are greater than the size of the projectile but smaller than that of the target.

In order to analyze the centrality dependence of the correlation effect, both the $p + Pb$ and $S + Pb$ data have been divided into three multiplicity bins, based on the charged-particle multiplicity measured by the silicon detector. The binning is chosen to give roughly equal proton-pair statistics in each sub-sample. The correlation functions corresponding to the three multiplicity selections are shown in Fig. 3 for $p + Pb$ and $S + Pb$. A systematic decrease of the correlation effect with increasing multiplicity is observed, corresponding to an increase in the size of the emitting volume. The r_o values indicate the scale of these changes.

The comparison of the data with the predictions of RQMD is shown in Fig. 4. In the case of $p + Pb$ collisions, the experimental data are well reproduced by the model. For $S + Pb$,

the model gives a somewhat larger correlation effect than is observed in the data. Fitting the $S + Pb$ RQMD prediction with the same Gaussian model (and same fraction of protons from Λ decay) as used for the data yields $r_o = \tau = 2.27^{+0.02}_{-0.02}$ fm, compared to $r_o = \tau = 2.65^{+0.19}_{-0.17}$ for the data.

5 Discussion

A simple, one-dimensional description with Gaussian co-moving sources is used to quantify the correlation effects. In introducing the co-moving source, it is assumed that particles with similar longitudinal velocities are emitted from nearby space-time points, such as occurs when fast longitudinal expansion takes place. In this case, the correlation function effectively measures only a part of the space-time extent of the emission volume. For the $S + Pb$ system, the multiplicity cuts select different impact parameter collisions, and hence different sizes of the overlapping region between projectile and target nucleons. This is reflected in the observed centrality dependence of the correlation functions. Comparison of the measured source sizes with the RMS radii of the projectile and the target is also in qualitative agreement with such an interpretation. Note that in the target fragmentation region the sizes measured by two-proton correlations reflect rather the size of the target nucleus [10]. In the case of $p + Pb$ collisions, the number of projectile participants is always equal to one and the measured size can be related to the extent of the hot region along the path of the proton in the lead nucleus. The source sizes in this case are much smaller than in the case of the sulphur projectile.

These data can be compared to correlation results obtained for other particle types near midrapidity and in similar p_T intervals, which assume the same type of emitting source. For both systems studied ($p + Pb, S + Pb$), the proton source sizes appear to be smaller than those of pions, especially in the case of the sulphur projectile: for $p + Pb$, $r_{Ts}(\pi^+) = 2.00 \pm 0.25$ fm while for $S + Pb$, $r_{Ts}(\pi^+) = 4.15 \pm 0.27$ fm ($\langle p_T \rangle \approx 150$ MeV/ c in both cases) [19, 20]. The r_o values for protons are similar to the corresponding kaon source sizes: for $p + Pb$, $r_{Ts}(K^+) = 1.22 \pm 0.76$ fm while for $S + Pb$, $r_{Ts}(K^+) = 2.55 \pm 0.20$ fm ($\langle p_T \rangle \approx 240$ MeV/ c in both cases) [18]. (Note that for the three-dimensional boson source parameters, multiplication by a factor of $\sqrt{3}$ is also necessary to obtain RMS sizes). The Gaussian source model used in these analyses describes sources for which the momenta and positions of the emitted particles are independent in the LCMS. Collision dynamics may, however, induce correlations between the measured source size and the transverse momentum of the particles. In particular, a decrease of the measured size with increasing transverse mass m_T (where $m_T = \sqrt{p_T^2 + m^2}$), observed in common for pions and kaons, may indicate the collective expansion of an equilibrated system formed during the collision [14, 19]. The smaller source sizes for the two-proton data ($\langle m_T \rangle \approx 970$ MeV) compared to the two-boson data [18, 19, 20] are in qualitative agreement with such an m_T dependence.

The contribution of indirect protons coming from hyperon decays is also a parameter in the description of the experimental results, and can influence the values of the extracted source sizes. The experimental uncertainty on the Λ yield is described above, and results

in a systematic error of approximately 0.2 fm on the extracted r_o parameters. Of the other hyperons, Monte Carlo studies show that only the Σ^+ also contributes to the proton yield measured in the NA44 spectrometer. RQMD and Venus predict that the number of detected protons from Σ^+ decay is at most 30% and 10%, respectively, of that from Λ decay - less than the experimental uncertainty on the Λ yield itself. Possible uncertainty in the contribution of indirect protons cannot significantly alter the conclusion on the size of the proton source compared to the pion source however, nor on the centrality dependence of the observed sizes. In order to produce the change in the measured correlation functions between the lowest and highest multiplicity bins assuming that the difference is due entirely to indirect protons implies that more than 50% of detected protons come from hyperon decays. However, an enhanced emission of hyperons with respect to that predicted by the RQMD model in the case of $S + Pb$ collisions may be responsible for the difference between the model prediction and the results of measurements.

6 Conclusion

These results demonstrate the first attempt to include baryon-baryon correlations in the analysis of the space-time dynamics of particle emission at midrapidity at CERN SPS energies. The measured source sizes increase with the mass of the projectile and with the collision multiplicity. Within the context of a Gaussian source model, the proton radius parameters are smaller than the size of the target nucleus but larger than the sizes of the projectiles. Comparing to other particle types, the proton size parameters are smaller than those for pions, and similar to those for kaons, measured in the same collisions. (Note that collision dynamics may induce a dependence of the measured source sizes on the momentum of the emitted particles.) Good agreement with the results of RQMD (v1.08) simulations is seen for $p + Pb$ collisions. For $S + Pb$ collisions, the measured correlation effect is somewhat weaker than that predicted by the model simulations.

7 Acknowledgements

The NA44 Collaboration wishes to thank the staff of the CERN PS-SPS accelerator complex for their excellent work. We thank the technical staff at CERN and the collaborating institutes for their valuable contributions. We are also grateful for the support given by the Science Research Council of Denmark; the Japanese Society for the Promotion of Science, and the Ministry of Education, Science and Culture, Japan; the Science Research Council of Sweden; the US Department of Energy and the National Science Foundation. We thank Dr. H. Sorge for the use of the RQMD code; Dr. K. Werner for the Venus code; and Drs. R. Lednický and S. Pratt for making their correlation codes available to us, and for fruitful discussions.

References

- [1] S.E. Koonin, Phys. Lett. **70B** (1977) 43.
- [2] R. Lednicky, V.L. Lyuboshitz, Yad. Fiz. **35** (1982) 1316 (Sov. J. Nucl. Phys. **35** (1982) 770).
- [3] S. Pratt, M.B. Tsang, Phys. Rev. **C36** (1987) 2390.
- [4] C. Ghisalberti *et al.*, Nucl. Phys. **A583** (1995) 401c.
- [5] T. Siemiarczuk, P. Zieliński, Phys. Lett. **24B** (1967) 675.
- [6] J. Pochodzalla *et al.*, Phys. Rev. **C35** (1987) 1695.
- [7] Z.Chen *et al.*, Phys. Rev. **C36** (1987) 2297.
- [8] H.A. Gustafsson *et al.*, Phys. Rev. Lett. **53** (1984) 544.
- [9] W.G. Gong *et al.*, Phys. Rev. **C43** (1991) 1804.
- [10] T.C. Awes *et al.*, Z. Phys. **C65** (1995) 207.
- [11] J. Bartke *et al.*, Z. Phys. **A324** (1986) 471.
- [12] S.A. Azimov *et al.*, Phys. Rev. **D29** (1984) 1304.
- [13] M.A. Lisa *et al.*, Phys. Rev. Lett. **70** (1993) 3709.
- [14] D.E. Fields *et al.*, Phys. Rev. **C52** (1995) 986.
- [15] I.G. Bearden *et al.*, Phys. Rev. **C57** (1998) 837.
- [16] I.G. Bearden *et al.*, Phys. Lett. **B388** (1996) 431.
- [17] H. Bøggild *et al.*, Phys. Lett. **B302** (1993) 510.
- [18] H. Beker *et al.*, Z. Phys. **C64** (1994) 209.
- [19] H. Beker *et al.*, Phys. Rev. Lett. **74** (1995) 3340.
- [20] H. Bøggild *et al.*, Phys. Lett. **B349** (1995) 386.
- [21] T. Alber *et al.*, Z. Phys. **C66** (1995) 77.
- [22] T. Alber *et al.*, Phys. Rev. Lett. **74** (1995) 1303.
- [23] H. Sorge, H. Stöcker and W. Greiner, Nucl. Phys. **A498** (1989) 567c.
- [24] W.A. Zajc *et al.*, Phys. Rev. **C29** (1984) 2173.
- [25] K. Werner, Phys. Rep. **232** Nb(2-5) (1993) 87.
- [26] M. Gaździcki, Nucl. Phys. **A590** (1995) 197c.
- [27] E.G. Judd, Nucl. Phys. **A590** (1995) 291c.
- [28] B.A. Brown *et al.*, Journ. of Phys. **G10** (1984) 1683.

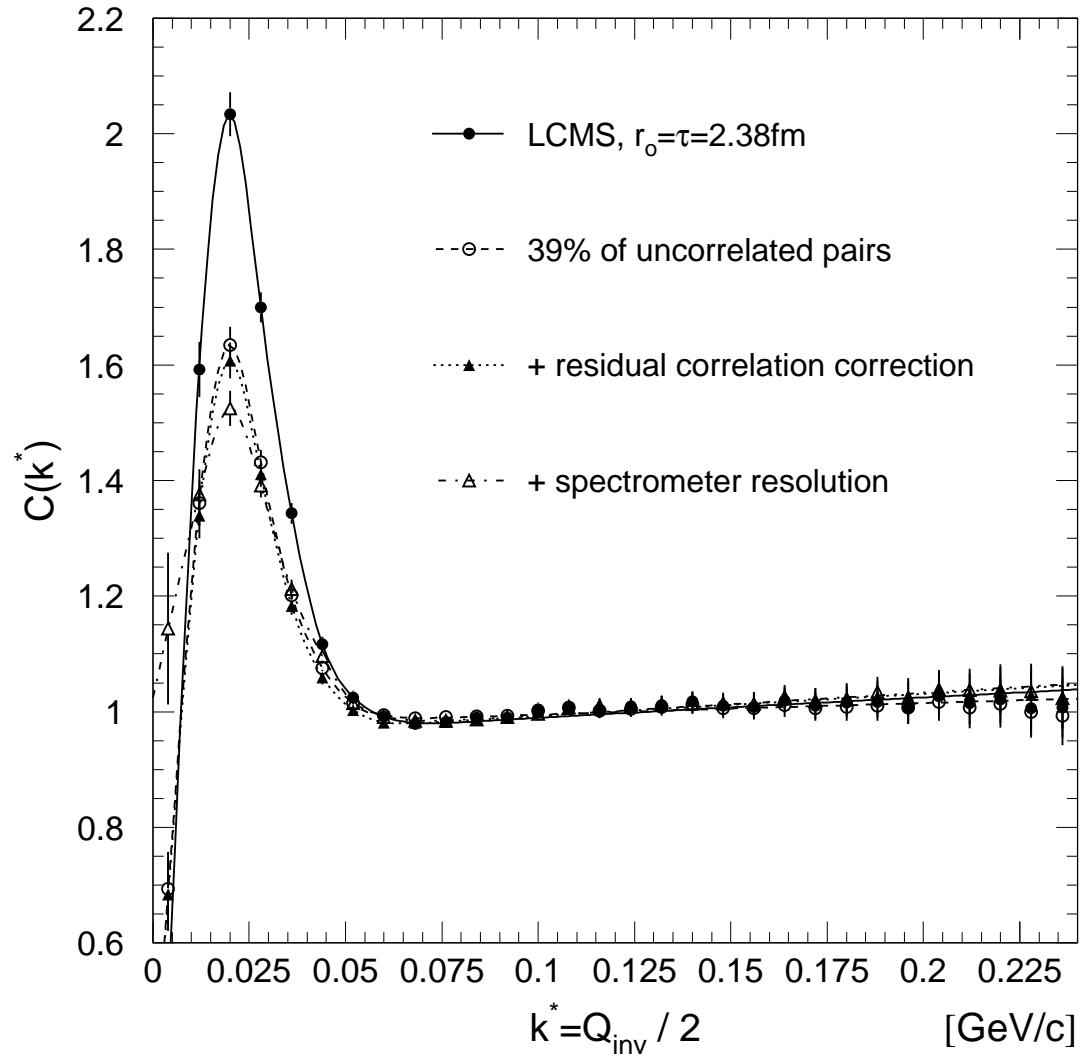


Figure 1: The influence of different experimental factors on the form of the measured correlation function. The example of a Gaussian source with $r_o = \tau = 2.38 \text{ fm}$ is shown, where the effect of each contribution has been added cumulatively.

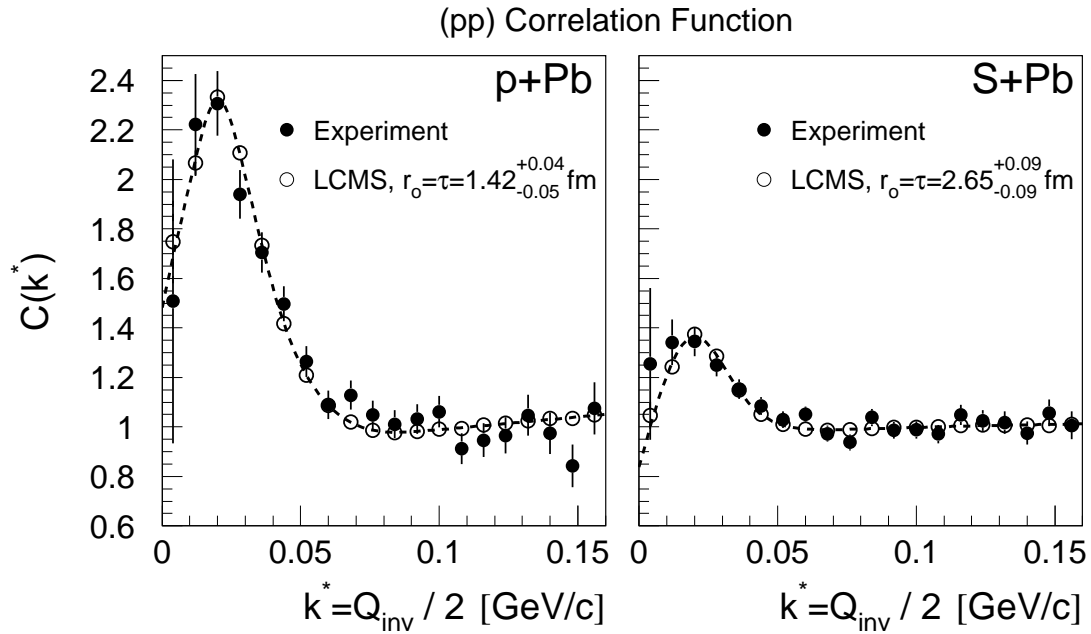


Figure 2: Two-proton correlation function for $p + Pb$ (left) and $S + Pb$ (right) collisions. The open points and dashed lines show the predicted correlation functions for longitudinally co-moving Gaussian sources with the radii indicated in the figure.

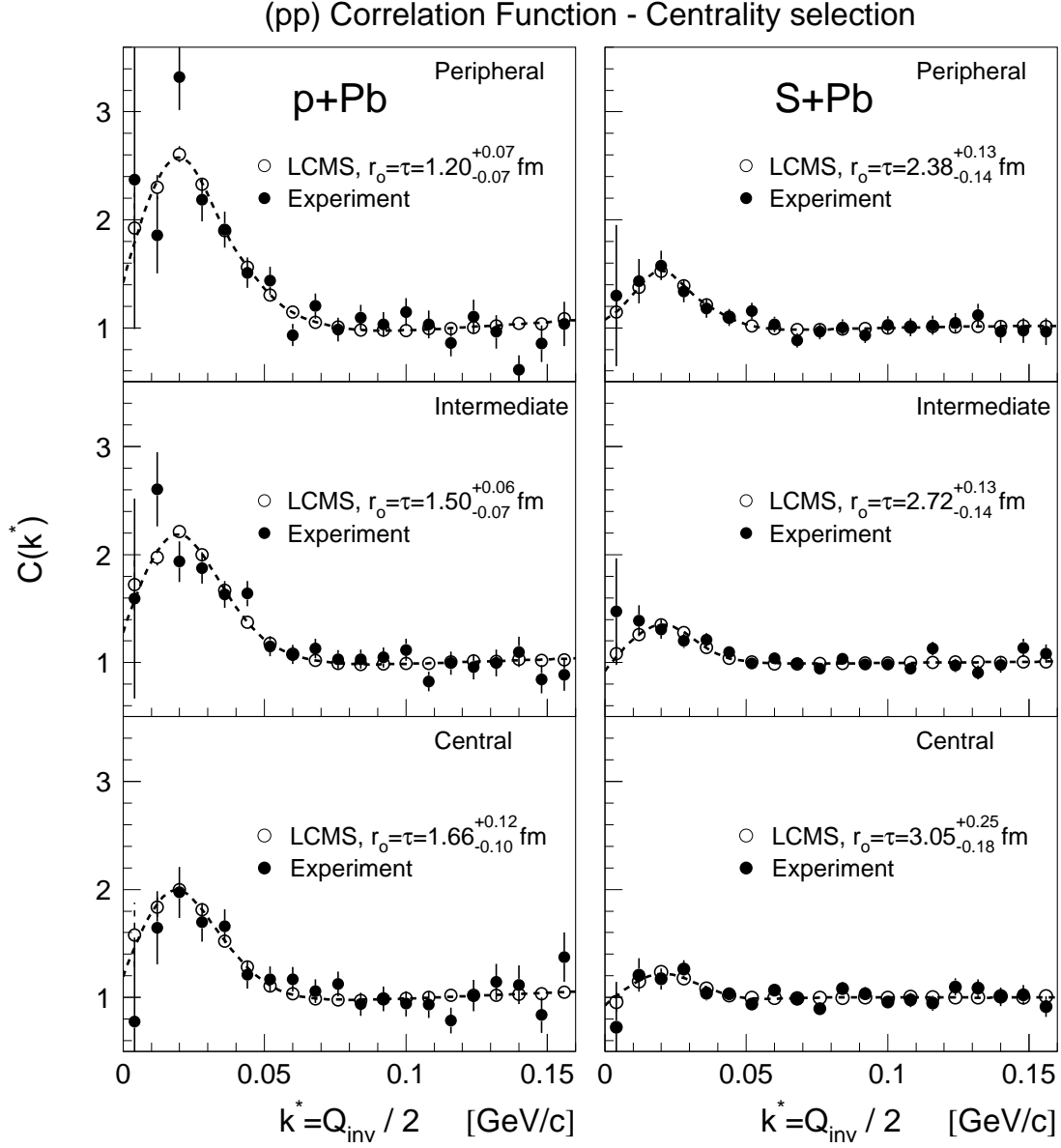


Figure 3: Two-proton correlation function for $p + Pb$ (left) and $S + Pb$ (right) collisions for three different multiplicity selections. The open points and dashed lines show the form of correlation function for longitudinally co-moving Gaussian sources with the radii indicated in the figure.

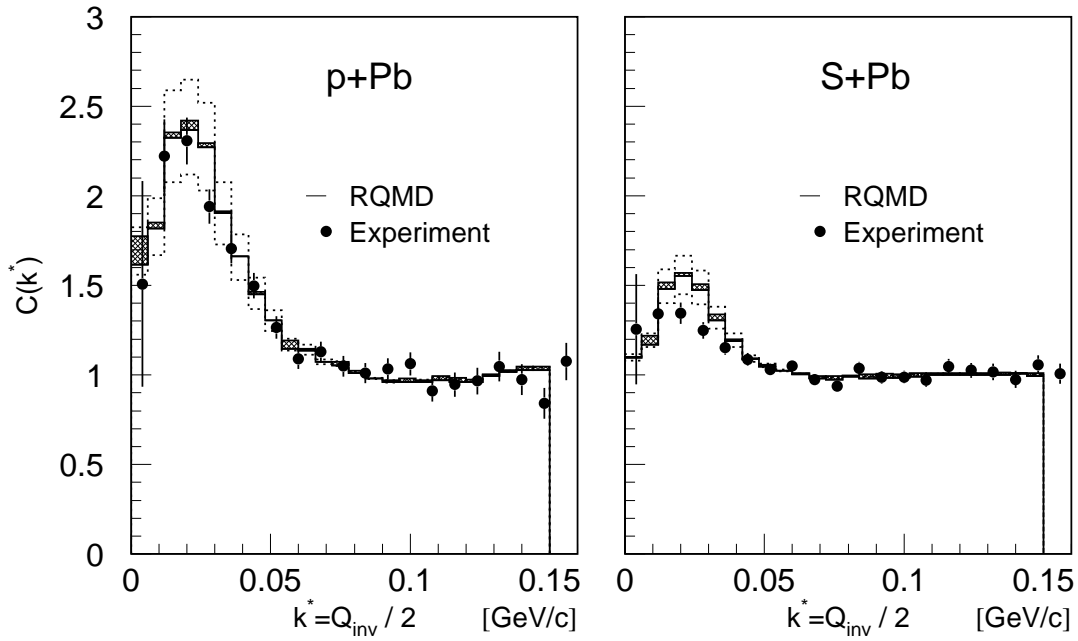


Figure 4: Comparison of the experimental correlation functions with predictions of the RQMD (v1.08) model for $p + Pb$ (left) and $S + Pb$ (right) collisions. The hatched error band on the RQMD predictions includes the systematic error due to the uncertainty in the spectrometer resolution and the uncertainty on the impact parameter weighting obtained by matching the multiplicity distributions of the data and the model. The non-hatched error band reflects the experimental uncertainty on the measured Λ yields [26, 27]. Statistical errors are negligible.